ACS Energy LETTERS

Cite This: ACS Energy Lett. 2019, 4, 2181−2184

http://pubs.acs.org/journal/aelccp

ENERGY EXPRESS

Energy Level Tuning at the $MAPbI_3$ Perovskite/Contact Interface Using Chemical Treatment

Daniele Meggiolaro,[*,†,‡] Edoardo Mosconi,[†] Andrew H. Proppe,[*,§,∥] Rafael Quintero-Bermudez,[∥] Shana O. Kelley,[§,⊥] Edward H. Sargent,[∥] and Filippo De Angelis[†,#]

[†]Computational Laboratory for Hybrid/Organic Photovoltaics (CLHYO), Istituto CNR di Scienze e Tecnologie Molecolari (ISTM-CNR), Via Elce di Sotto 8, 06123 Perugia, Italy

[‡]CompuNet, Istituto Italiano di Tecnologia, Via Morego 30, 16163 Genova, Italy

[§]Department of Chemistry, University of Toronto, Toronto, Ontario, Canada M5S 3G4

[∥]The Edward S. Rogers Department of Electrical and Computer Engineering, University of Toronto, Toronto, Ontario, Canada M5S 3G4

[⊥]Department of Pharmaceutical Sciences, Leslie Dan Faculty of Pharmacy, University of Toronto, Toronto, Ontario, Canada M5S 3M2

[#]Department of Chemistry, Biology and Biotechnology, University of Perugia, Via Elce di Sotto 8, 06123 Perugia, Italy

Supporting Information

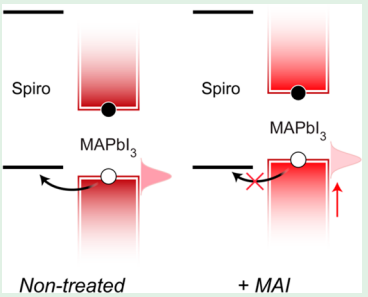

ABSTRACT: Metal halide perovskites are rivaling established materials for thin film photovoltaics. Being able to tune interfacial alignment of energy levels may allow a further boost to the efficiency of perovskite optoelectronic devices. By using Density Functional Theory (DFT) modeling and experimental analysis, we show that the band edge energies of the prototypical $MAPbI_3$ (MA = methylammonium) perovskite can in principle be varied by as much as 1 eV via postsynthetic chemical treatment. In particular, MAI-rich (PbI_2-rich) surfaces induce an energy upshift (downshift) of the perovskite band energies, and this can either inhibit or favor hole transfer at the perovskite/HTL interface.

Metal halide perovskites have demonstrated high solar cell efficiencies due to their outstanding optoelectronic properties.[1,2] The efficiencies of polycrystalline thin films, however, are influenced by surfaces where the diffusion of charges toward the selective contacts takes place. Favorable band alignments at the perovskite/charge transport layer interface and low surface recombination rates are crucial factors in order to reduce the current leakage and improve the overall efficiency of solar cells. Although the development of specialized carrier-selective contacts for perovskite active layers has proven to be an effective strategy to reduce surface recombination,[3] large efficiency variations have been reported for different perovskite preparation techniques using the same selective contacts, indicating a strong dependence of the electronic and optical properties on the perovskite morphology, crystal size, and chemical composition of the film.[4,5] Deviations from the nominal stoichiometry, in fact, affect the chemical composition of the surfaces, their defect chemistry, and the associated electronic properties.[4] Emara et al. investigated the ionization energies (IEs) of several $MAPbI_3$ films of different nominal chemical composition by X-ray photoemission spectroscopy (XPS),[6] finding different IEs for films of different stoichiometry that ranged from 5.7 to 6.4 eV.[6] Such large variations of the surface energy levels have a strong impact on the diffusion of charges at the interface and open the possibility to develop innovative chemical treatments aimed at improving the efficiency of solar cell devices.

In this paper, we investigate the stability and electronic properties of differently terminated surfaces of $MAPbI_3$ by focusing on the potential impact that deviations from stoichiometry and chemical treatments can have on the charge extraction capacity at the perovskite interface with hole-selective contacts. The stability and electronic properties of $MAPbI_3$(001) surfaces have been studied by DFT, increasing the MAI coverage (θ) from 0 to 1 (see the SI for details). The structures of representative slabs for θ = 0, 0.5, and 1 are reported in Figure 1d−f.

Received: July 23, 2019
Accepted: August 14, 2019
Published: August 14, 2019

DOI: 10.1021/acsenergylett.9b01584
ACS Energy Lett. 2019, 4, 2181−2184

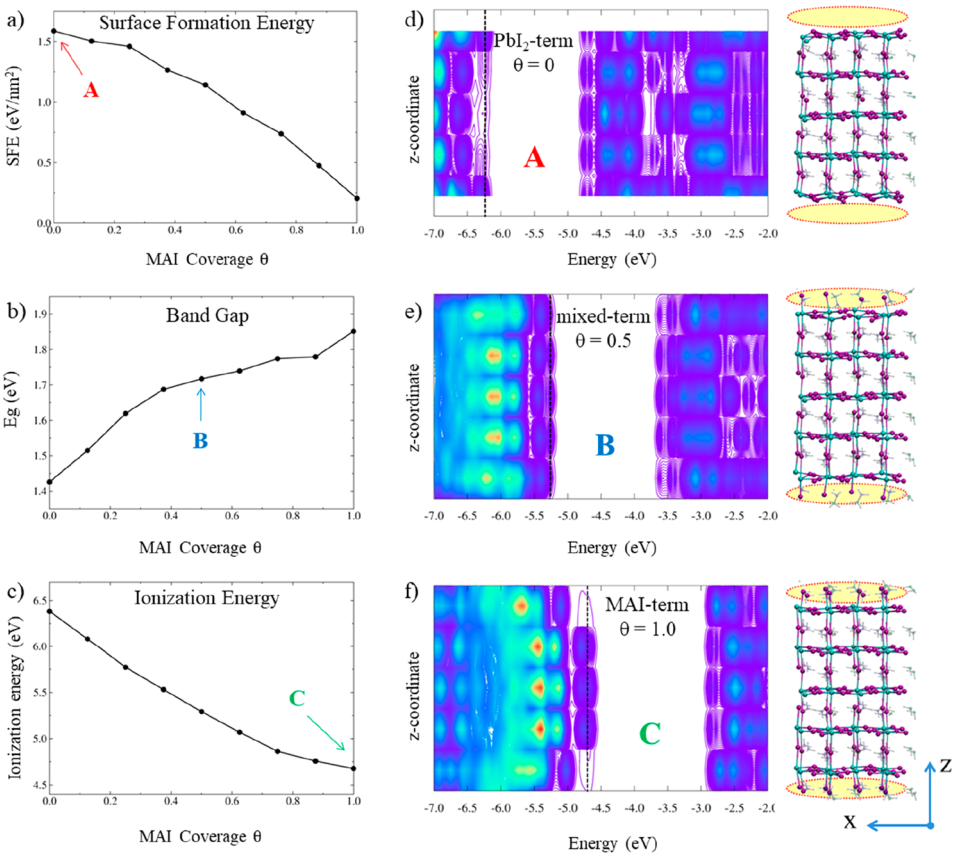

Figure 1. Evolution of the (a) SFE (PBE-D3); (b) band gap (PBE) and (c) IE (HSE06-SOC, α = 0.43) vs the MAI coverage θ of the (001) surface; (d–f) isodensity contour plots of the projected DOS (PBE) for representative points A, B, and C, i.e., MAI coverage θ of 0, 0.5, and 1.0, respectively, with the associated structures. Blue (red) regions correspond to low (high) DOS.

In Figure 1a, the calculated surface formation energies (SFEs) for the modelled slabs are plotted as a function of MAI coverage θ (see Table S1), highlighting the higher stability, i.e., lower SFE, of the MAI-terminated over the flat PbI_2-terminated (001) surface; the SFE decreases almost linearly with the MAI coverage, consistent with calculations by Haruyama et al.[7] The calculated IE, i.e., the energy required to remove one electron from the top of the valence band (see SI), and the associated band gaps are reported in Figure 1b,c. IEs show a linear increase by decreasing the MAI coverage due to a progressive decrease of the valence band maximum (VBM) energy, which is also associated with a slight decrease of the band gap. This behavior is portrayed in the projected density of states (DOS) aligned to the vacuum levels reported in Figure 1d–f. Moving from PbI_2- to MAI-terminated surfaces, a remarkable upshift of both the VBM and CBM is observed. The deepening of the VB by increasing the lead content (structure C → A) leads to the emergence of surface states localized on the outer PbI_2 layers (see Figure S1).

To investigate experimentally the predicted trend of IE vs MAI coverage of the surface, we carried out ultraviolet photoelectron spectroscopy (UPS) on polycrystalline $MAPbI_3$ of different chemical compositions. Polycrystalline samples were post-treated with solutions of PbI_2 and MAI dissolved in isopropanol to reduce damage to the film. The average chemical composition of the surface was probed by XPS (see Table S6) to monitor the effectiveness of the treatments. The VBMs of these $MAPbI_3$ films were then measured by using UPS. Results are reported in Table S2 and Figure S2 for each treatment (details of these measurements and extraction of the IE and VBM can be found in the SI). The pristine $MAPbI_3$ perovskite film shows a VBM placed at 5.7 eV below the vacuum. A post-treatment leads to an excess of ∼10% of PbI_2 surfaces over MAI surfaces and yields a VBM decrease of 0.1 eV. A significantly more pronounced effect is reported for MAI treatments of pristine $MAPbI_3$. The VBM increases by up to 1.3 eV in the cases when MAI surfaces increase by 50% with respect to the nontreated surface. The limited increase of the IE upon PbI_2 treatment compared to the MAI treatment suggests that the addition of PbI_2 is less effective in tuning the chemical composition of the surface. This is likely due to the limited stability of PbI_2-terminated surfaces compared to MAI-terminated surfaces, as found by our calculations.

It should be noted that the VBM shifts discussed do not manifest as a shift of the entire valence spectra; in the low kinetic energy (high binding energy) part of the spectrum, there are two discernible photoemission intensity drop-offs (indicated by arrows in Figure S2). This would suggest that the film consists of both band-shifted and unshifted components. This might be attributed to the limitations of the MAI treatment, which may be successful only in parts of the film with exposed PbI_2 facets. The VBMs reported for the post-treated films were extracted using the secondary photoemission intensity drop-off.

These results, which agree well with DFT trends, are in good agreement with work of Emara et al. on MAPI films, where lower IEs and higher valence DOSs have been reported for low

DOI: 10.1021/acsenergylett.9b01584
ACS Energy Lett. 2019, 4, 2181–2184

Pb/N chemical ratios (MAI-rich surfaces) and stoichiometric surfaces.[6] As discussed by these authors,[6] variations in the composition of the film do not introduce in-gap states, but they are mostly associated with variations in the DOS of the VB.[6]

The change in the VBM energy upon MAI exposure has a profound impact on the hole extraction properties at the perovskite/hole transport layer (HTL) interface. In Figure 2a,

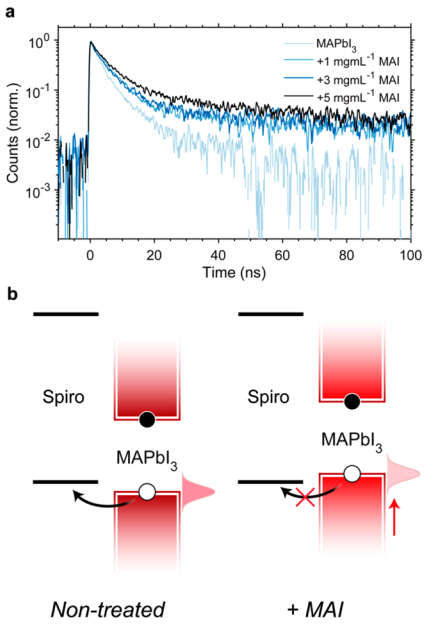

Figure 2. Experimental observation of the VBM shift for MAI-treated and nontreated (control) $MAPbI_3$ surfaces in contact with a spiro-OMeTAD hole-selective layer: (a) PL lifetimes of nontreated and MAI-treated surfaces, highlighting longer carrier lifetimes for the MAI-treated surface; (b) schematic of the VB alignment between spiro and $MAPbI_3$ with and without MAI treatment. Details of the experimental conditions used can be found in the SI.

the photoluminescence (PL) intensity measured over time for four differently treated $MAPbI_3$ films contacted with a spiro-OMeTAD HTL is reported. MAI-treated films show a longer PL decay compared to nontreated films, indicating that quenching by spiro-OMeTAD (via hole extraction from the perovskite) is effectively reduced and that recombination of holes with electrons occurs on longer time scales. This behavior can be easily explained by considering the band energy alignment at the $MAPbI_3$/spiro-OMeTAD interface, whereby the MAI treatment induces an energy upshift of the VBM of the perovskite, creating an unfavorable band mismatch at the interface that limits the hole transfer process, Figure 2b. This would be consistent with holes accumulating in the perovskite, causing them to recombine on longer time scales compared to the nontreated surface, where they are more easily extracted at the interface, leading to quenching of the PL. We note that in the absence of the spiro-OMeTAD layer, increasingly concentrated MAI treatments actually decrease the PL lifetime (see Figure S3), indicating that the longer lifetimes observed with the spiro-OMeTAD HTL arise due to changes in the interfacial charge extraction rate and not simply due to surface passivation by excess MAI.

On the basis of these results, PbI_2-rich environments promote hole transfer at the perovskite/HTL interface by stabilizing the VB of the perovskite and leading to an optimal matching of the band edges at the interface. On the other hand, the use of an excess of MAI results in an unfavorable band alignment with the HTL, although it is beneficial in increasing the DOS of the perovskite at the interface and may favor electron injection at electron-selective contacts. PbI_2 addition has generally been reported to increase the performance of perovskites solar cells[8,9] due to defect passivation at grain boundaries and the increased interfacial coupling at the TiO_2/perovskite interface.[9,10]

The addition of MAI, on the other hand, in addition to hindering hole transfer at the HTL interface, decreases the lifetimes of photogenerated carriers (see Figure S3). The detrimental impact on the charge carrier lifetimes can be ascribed to the increased density of iodine interstitial charge traps incorporated in the perovskite upon MAI treatment.[11,12]

Although the addition of PbI_2 is beneficial for increasing the performance of solar cells, it has detrimental effects on the photostability of perovskites[13] by promoting the expulsion of molecular iodine at the grain boundaries responsible for quenching of the PL properties and the lattice degradation.[13,14] The stabilization of lead ions at the surface by using passivating polymers or coordination ligands containing oxygen, such as PEO or TOPO, has been demonstrated as a successful strategy in order to reduce the charge trap density at the interface and to enhance the stability of perovskite solar cells against light and moisture.[14,15] We modeled the PbI_2-terminated surface with an adsorbed layer of H_2O molecules as representative of PEO and TOPO adsorbents (see Figure S1). H_2O forms a monolayer that leads to a ~ 0.7 eV decrease in IE (Table S1), with limited impact on the band gap of the surface. The water-induced VB upshift is substantially lower than that obtained by the same MAI coverage, indicating that passivation of surface lead atoms with oxygen-containing functional groups can be a successful strategy in order to improve the photostability of $MAPbI_3$ without compromising the charge extraction capacity at the HTL interface.

■ ASSOCIATED CONTENT

Supporting Information

The Supporting Information is available free of charge on the ACS Publications website at DOI: 10.1021/acsenergylett.9b01584.

Computational details, calculated surface quantities, average chemical compositions, convergence tests, XPS elemental ratio analysis, PL lifetimes, UPS results, and HOMO orbitals of the (001) surfaces (PDF)

■ AUTHOR INFORMATION

Corresponding Authors

*E-mail: daniele.meggiolaro@iit.it (D.M.).
*E-mail: andrew.proppe@mail.utoronto.ca (A.P.).

ORCID

Daniele Meggiolaro: 0000-0001-9717-133X
Rafael Quintero-Bermudez: 0000-0002-4233-395X
Shana O. Kelley: 0000-0003-3360-5359
Edward H. Sargent: 0000-0003-0396-6495
Filippo De Angelis: 0000-0003-3833-1975

Notes

The authors declare no competing financial interest.

DOI: 10.1021/acsenergylett.9b01584
ACS Energy Lett. 2019, 4, 2181−2184

■ ACKNOWLEDGMENTS

The research leading to these results received funding from the European Union's Horizon 2020 research and innovation program under Grant Agreement No. 764047 of the ESPRESSO project. The Ministero dell'Istruzione dell'Università e della Ricerca (MIUR) and Università degli Studi di Perugia are acknowledged for financial support through the program "Dipartimenti di Eccellenza 2018-2022" (Grant AMIS) to F.D.A.

■ REFERENCES

(1) Stranks, S. D.; Eperon, G. E.; Grancini, G.; Menelaou, C.; Alcocer, M. J. P.; Leijtens, T.; Herz, L. M.; Petrozza, A.; Snaith, H. J. *Science* **2013**, *342*, 341−344.
(2) Miyata, A.; Mitioglu, A.; Plochocka, P.; Portugall, O.; Wang, J. T.-W.; Stranks, S. D.; Snaith, H. J.; Nicholas, R. J. *Nat. Phys.* **2015**, *11*, 582−587.
(3) Tvingstedt, K.; Gil-Escrig, L.; Momblona, C.; Rieder, P.; Kiermasch, D.; Sessolo, M.; Baumann, A.; Bolink, H. J.; Dyakonov, V. *ACS Energy Lett.* **2017**, *2*, 424−430.
(4) Fassl, P.; Lami, V.; Bausch, A.; Wang, Z.; Klug, M. T.; Snaith, H. J.; Vaynzof, Y. *Energy Environ. Sci.* **2018**, *11*, 3380−3391.
(5) Murali, B.; Dey, S.; Abdelhady, A. L.; Peng, W.; Alarousu, E.; Kirmani, A. R.; Cho, N.; Sarmah, S. P.; Parida, M. R.; Saidaminov, M. I.; et al. *ACS Energy Lett.* **2016**, *1*, 1119−1126.
(6) Emara, J.; Schnier, T.; Pourdavoud, N.; Riedl, T.; Meerholz, K.; Olthof, S. *Adv. Mater.* **2016**, *28*, 553−559.
(7) Haruyama, J.; Sodeyama, K.; Han, L.; Tateyama, Y. *J. Phys. Chem. Lett.* **2014**, *5*, 2903−2909.
(8) Merdasa, A.; Kiligaridis, A.; Rehermann, C.; Abdi-Jalebi, M.; Stöber, J.; Louis, B.; Gerhard, M.; Stranks, S. D.; Unger, E. L.; Scheblykin, I. G. *ACS Energy Lett.* **2019**, *4*, 1370−1378.
(9) Mosconi, E.; Grancini, G.; Roldán-Carmona, C.; Gratia, P.; Zimmermann, I.; Nazeeruddin, M. K.; De Angelis, F. *Chem. Mater.* **2016**, *28*, 3612−3615.
(10) Wang, L.; McCleese, C.; Kovalsky, A.; Zhao, Y.; Burda, C. *J. Am. Chem. Soc.* **2014**, *136*, 12205−12208.
(11) Meggiolaro, D.; De Angelis, F. *ACS Energy Lett.* **2018**, *3*, 2206−2222.
(12) Park, J.-S.; Calbo, J.; Jung, Y.-K.; Whalley, L. D.; Walsh, A. *ACS Energy Lett.* **2019**, *4*, 1321−1327.
(13) Liu, F.; Dong, Q.; Wong, M. K.; Djurišić, A. B.; Ng, A.; Ren, Z.; Shen, Q.; Surya, C.; Chan, W. K.; Wang, J.; et al. *Adv. Energy Mater.* **2016**, *6*, 1502206.
(14) Motti, S. G.; Meggiolaro, D.; Barker, A. J.; Mosconi, E.; Perini, C. A. R.; Ball, J. M.; Gandini, M.; Kim, M.; De Angelis, F.; Petrozza, A. *Nat. Photonics* **2019**, *13*, 532−539.
(15) Kim, M.; Motti, S. G.; Sorrentino, R.; Petrozza, A. *Energy Environ. Sci.* **2018**, *11*, 2609−2619.

DOI: 10.1021/acsenergylett.9b01584
ACS Energy Lett. 2019, 4, 2181−2184